Transformation of nitrogen during solar pyrolysis of algae in molten salt

Jing Peng, Jun Li, Dian Zhong, Kuo Zeng, Kang Xu, Junjie Gao, Ange Nzihou, Xiong Zhang, Haiping Yang, Hanping Chen

Transformation of nitrogen during solar pyrolysis of algae in molten salt

Jing Peng [a,1], Jun Li [b,1], Dian Zhong [b], Kuo Zeng [a,b,*], Kang Xu [a], Junjie Gao [b], Ange Nzihou [c,d], Xiong Zhang [b,*], Haiping Yang [b], Hanping Chen [b]

[a] China-EU Institute for Clean and Renewable Energy, Huazhong University of Science and Technology, Wuhan 430074, China
[b] State Key Laboratory of Coal Combustion, School of Energy and Power Engineering, Huazhong University of Science and Technology, Wuhan 430074, China
[c] Universit´e de Toulouse, IMT Mines Albi, RAPSODEE CNRS UMR 5302, Campus Jarlard, F.81013 Albi Cedex 09, France
[d] Andlinger Center for Energy and the Environment, Princeton University, Princeton, NJ 08544, USA

A B S T R A C T

Molten salt pyrolysis of N-rich algae driven by concentrated solar energy is considered as an economical and environmentally friendly method to prepare N-doped value-added carbon. The transformation of nitrogen during the carbon production process by algae pyrolysis in molten Na_2CO_3-K_2CO_3 is investigated in-depth, which contributes to the utilization or treatment of nitrogen-containing products. Algae-N is mainly converted to gas—N, and the gas-N yield increases as temperature rises, reaching 75.7 wt.% at 900 °C. Molten salt reduces the release temperature of all N-containing gas, captures 89.6% of HCN as CN^- , and promotes the release of NH_3 and NO. The char-N is dominated by pyrrole-N and quaternary-N at 800–900 °C due to the promotion of molten salt and higher temperature. The major contributors to the bio-oil-N yield are pentadecanenitrile, isoamyl cyanide, benzyl nitrile, styryl cyanide, pyrrole and indole. Nitriles and indoles are promising N-containing products in value-added carbon production, while NH_3 and NO are primary pollution gas to be controlled.

1. Introduction

Serious environmental problems and fossil fuel depletion have led to increasing global interest in clean sustainable energy [1]. Among the alternative renewable resources, biomass has proven to be one of the potential sources that best meet global demand [2]. Algal biomass, as the third-generation biofuel, has many commercial applications in the energy, agriculture, chemical and other industries for its short growth cycle, wide distribution and strong char sequestration ability [3,4]. In recent years, the thermochemical transformation of algal biomass to produce solid, liquid, and gas biofuels has attracted more and more attention [5,6].

In general, the large-scale thermochemical processes for algal biomass consist mainly of liquefaction, pyrolysis and gasification [7]. Algae liquefaction typically operates at temperatures of 300–350 °C and pressures of 5–20 MPa. It has the advantage of making full use of the entire algae, but suffers from the safety risks and operating costs associated with higher pressure [8–10]. Algae pyrolysis is usually carried out at temperatures between 400 and 600 °C, and this moderate temperature facilitates the production of bio-oil up to 80 wt% [11]. Nevertheless, bio-oil derived from pyrolysis are complex, unstable, viscous and high in oxygen and nitrogen [12]. The gasification process for syngas production can be mainly divided into supercritical gasification (600–1000 °C, 22.1–40 MPa) and conventional gasification (800–1000 °C, 101.32 kPa) [13]. However, constraints such as high pressure, high mineral or ash content and high CO_2 content in the gas product limit the promotion of gasification [14,15].

Nowadays, value-added carbon production from algal biomass is becoming attractive, as algae is a low-cost carbon and nitrogen resource [16,17]. Among the applications of value-added carbon, the capacitive carbon holds promise in energy storage systems. Typically, carbon produced from thermochemical conversion requires activation by additional activators such as KOH, $ZnCl_2$ and KNO_3 to enhance its surface functionalities or other features, ultimately improving its charge storage applications [18,19]. However, these alkali and salts are highly corrosive, toxic or thermally unstable [20]. On these issues, attempts have been made to produce value-added capacitive carbon by applying mild carbonate as activator. Several researchers have successfully obtained activated carbons (ACs) with considerable capacitance from peanut shell [17], bamboo shell [21], firewood [22] and tobacco stem

* Corresponding authors at: State Key Laboratory of Coal Combustion, School of Energy and Power Engineering, 1037 Luoyu Road, Wuhan 430074, Hubei, China.
E-mail addresses: zengkuo666@hust.edu.cn (K. Zeng), zhangxiong107@163.com (X. Zhang).
[1] Co-first authors.

Table 1
Properties of Spirulina platensis studied in this work.

Ultimate analysis (wt.%, d)					Proximate analysis (wt.%, d)		
C	H	N	S	O*	Volatile	Ash	Fixed carbon
47.22	6.43	10.87	1.97	26.01	77.09	7.50	15.41

d, dry basis; *, calculated by difference.

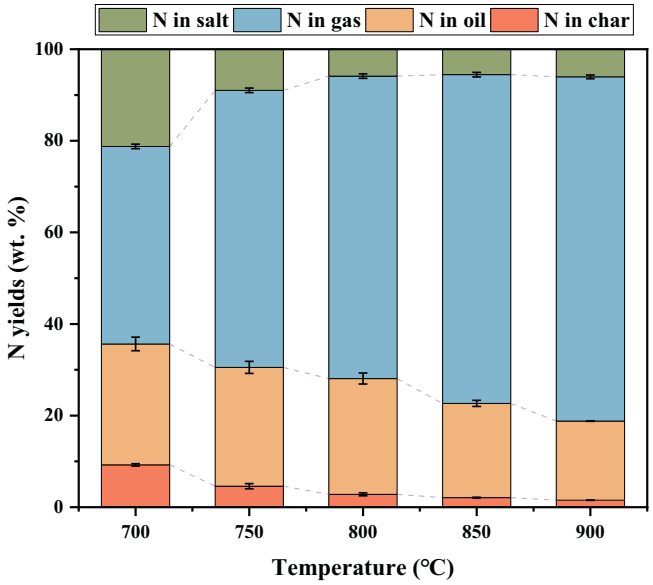

Fig. 1. Nitrogen distribution in pyrolysis products and molten salt.

[23] by using molten Na_2CO_3-K_2CO_3.

In our recent study, the molten salt (Na_2CO_3-K_2CO_3) pyrolysis of N-rich Spirulina platensis driven by concentrated solar energy is considered as an economical and environmentally friendly method to prepare capacitive carbon due to the sustainable, clean and renewable nature of solar energy and biomass [24]. However, despite the high specific surface area, capacitance and certain nitrogen content of the obtained ACs, the nitrogen was not enriched to a large extent in ACs as described in other studies using molten salt [17,21]. It indicates that nitrogen-containing substances are retained or transformed by the molten Na_2CO_3-K_2CO_3, which differs from that in other molten salt systems. On the other hand, as by-products during the ACs production process by algae pyrolysis, the generation of nitrogen-containing liquids and gases presents both opportunities and challenges [25]. Liquid products can be processes as valuable chemicals, such as pharmaceuticals, agrochemicals and industrial solvent [26], while the potential nitrogen pollution (toxic substances, photochemical smog, acid rain et.) caused by gas products could not be ignored either [27–30]. Therefore, it is necessary to investigate the transformation of nitrogen during the ACs preparation by algae pyrolysis in molten Na_2CO_3-K_2CO_3.

To the best of our knowledge, there are few studies investigated the nitrogen transformation during the algae pyrolysis in molten carbonates. Wei et al. [31] conducted seaweed pyrolysis in ternary molten carbonates (Li_2CO_3-Na_2CO_3-K_2CO_3), they declared that the nitrogen-containing compounds in bio-oil were reduced by nearly half. Recently, our group [32] studied the effect of molten carbonates (Li_2CO_3-Na_2CO_3-K_2CO_3) on the light and heavy fractions of pyrolysis bio-oil and found that the depolymerization of nitrogen-containing compounds in heavy bio-oil was promoted. However, the temperature for bio-oil production from algae pyrolysis is much lower (100–300 °C) than that for ACs production. In addition, these studies only focused on the properties of nitrogen-containing species in bio-oil and not on the interconversion of nitrogen-containing species in bio-oil, gas, biochar and salt.

In this study, the nitrogen transformation during algae pyrolysis in molten Na_2CO_3-K_2CO_3 are investigated with N-rich Spirulina platensis. The effect of molten Na_2CO_3-K_2CO_3 on the conversion pathways of N-containing compounds among bio-oil, gas and solid products, as well as molten salt is firstly obtained.

2. Materials and methods

2.1. Materials

The protein-rich Spirulina platensis (SP) purchased from Qingdao Haixingyuan Biology Technology Co., LTD is dried for 20 h in a 105 °C oven and then sieved (< 30 μm) before experiments. The ultimate analysis performed by the CHNS/O elemental analyzer (Vario Micro Cube, Germany) and proximate analysis based on GB/T 28731–2012 are shown in Table 1. The nitrogen content is 10.87 wt.%, and the ash content is 7.5 wt.%.

The alkali carbonates (Na_2CO_3 and K_2CO_3, analytical purity >99%) are purchased from the Sinopharm Chemical Reagent Co., LTD (Shanghai, China). The well-mixed Na_2CO_3-K_2CO_3 binary salts with a mass ratio of 1.1:1 is prepared using a planetary ball mill (PM 100, Germany) operating at a speed of 400 r/min for 34 min, of which the melting points are about 709 °C [17].

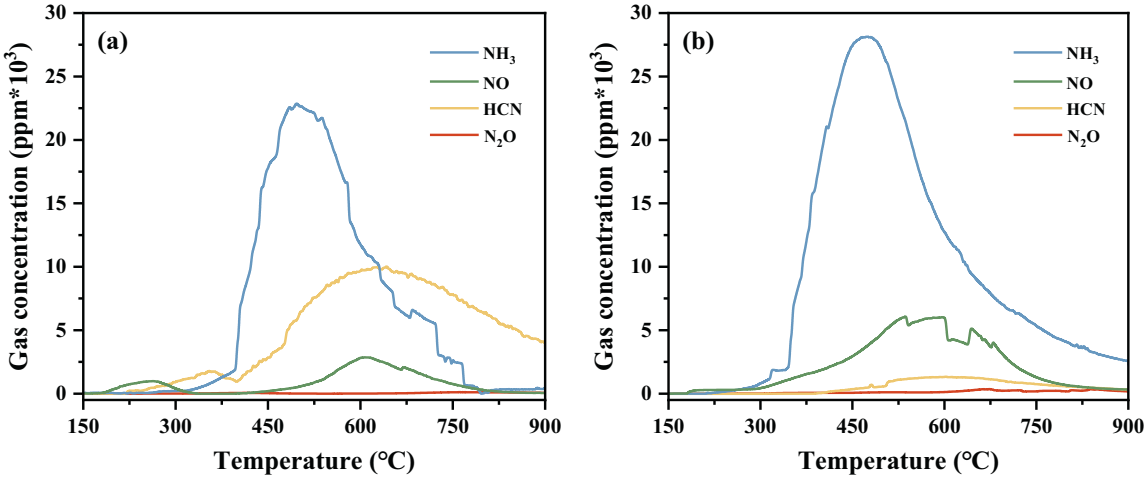

Fig. 2. Releasing curves of N-containing gases during pyrolysis: (a) without molten salt, (b) with molten salt.

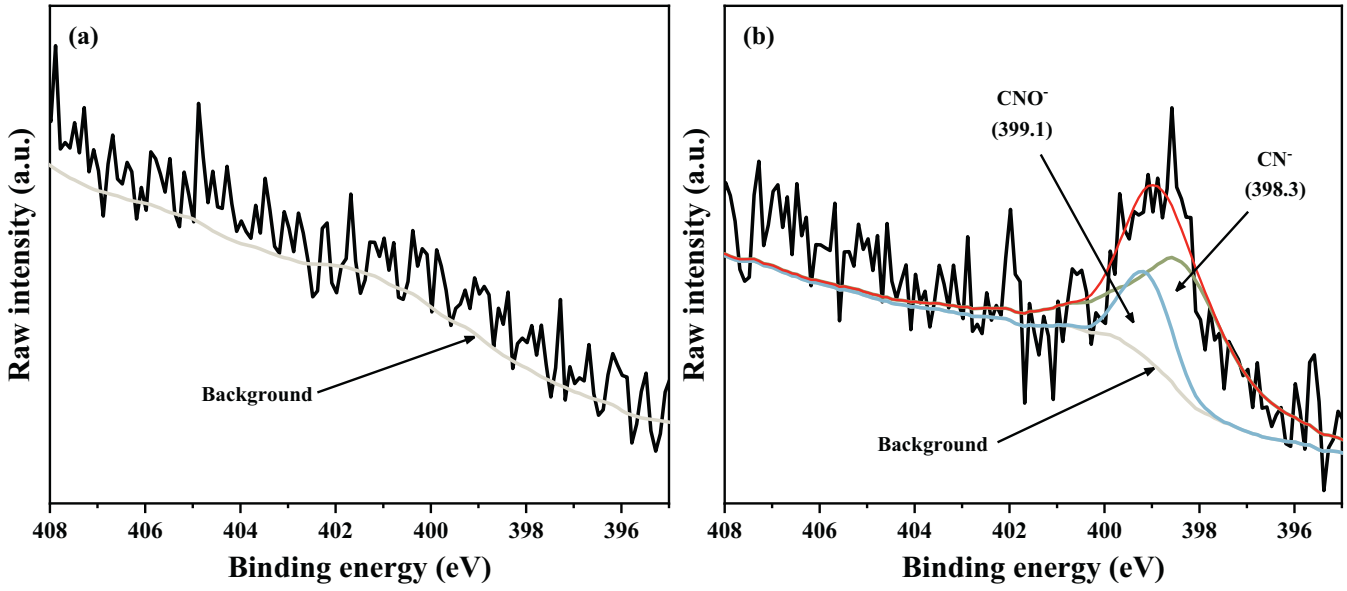

Fig. 3. High-resolution XPS N1s spectra of molten salt at 800 °C: (a) before reaction, (b) after reaction.

2.2. Experimental apparatus and procedure

The pyrolysis experiments are carried out in a vertical tubular quartz reactor of 60 mm in inner diameter and 600 mm in length, as shown in Fig. S1. And other necessary units, such as gas supply unit, product collection unit and product analysis unit are equipped.

Before each trial, 2 g algae and 20 g alkali carbonates are mixed uniformly to ensure sufficient contact in advance and loaded into the corundum crucible, and then hung together in the heating zone of the electric furnace with a stainless-steel wire. N_2 is introduced into the reactor with a flow rate of 200 mL/min for 30 mins to create an oxygen-free condition before the reaction began. Next, the mixture of algae and salts is heated to the targeted temperatures (700, 750, 800, 850 and 900 °C) in an hour and kept at the target temperatures for another one hour. The generated pyrolysis volatiles are brought out of the reactor by the carrier gas, the condensable components (refers to bio-oil) are cooled by the ice-water bath, and the non-condensable gases are analyzed online by a portable infrared gas analyzer. Finally, the corundum crucible is cooled down under N_2 atmosphere. Experiments under each parameter condition were repeated at least three times with a relative error of no more than 5%. All the data in this study were averaged with the results of multiple experiments.

In order to obtain the char product, the corundum crucible containing the mixture is first immersed in a beaker containing 1 M HCl for 4 h to remove the remaining carbonates and part of ash in raw algae. The mixed solution composed of HCl, chlorate and solid particles is then vacuum filtered using deionized water for six times, the as-received char is further vacuum-dried at 85 °C for 12 h and weighted to obtain the char yield. The final ACs is denoted as X-T, where X represents the reaction medium (A: without medium, B: Na_2CO_3-K_2CO_3) and T represents the target temperature (700, 750, 800, 850 and 900 °C). The nitrogen species in char, bio-oil and molten salt are analyzed by XPS, GC–MS and CHNS/O elemental analyzer after sampling, and the mass of nitrogen in char and bio-oil are obtained from the result of CHNS/O elemental analyzer.

2.3. Fourier transform infrared analysis

The characteristics of nitrogen-containing gases released in real time during pyrolysis is obtained by an on-line portable Fourier infrared gas analyzer (GASMET Dx4000, Temet, Finland), of which the measurement error was less than ±2%. The resolution of its interferometer is 8 cm^{-1} and the scanning speed is 10 times/s. The detector is MCT (Peltier refrigeration) with mid-infrared full spectrum range from 900 to 4200 cm^{-1}, and 180 °C is the working temperature of the sample chamber. Before measurement, the analyzer was zero calibrated using N_2, and it was checked to determine the presence of near-zero results. It should be mentioned that the mass of nitrogen in gas is obtained by the integration of the gas release curve.

2.4. GC–MS analysis

Nitrogen compounds in bio-oil are analyzed using a gas chromatography-mass Spectrometer (GC–MS, Agilent, 7890A/5975C) equipped with a TriPlus RSH™ auto sampler. The GC is fitted with a 30 m × 0.25 mm × 0.25 μm capillary column (Agilent: HP-5MS, 19,091 s-433). More detailed information of the instrument has been reported in our previous work [33].

2.5. XPS analysis

Nitrogenous functional groups in raw algae and its corresponding char products are analyzed by an X-ray photoelectron spectrometer (Thermo Scientific K-Alpha, USA) equipped with a monochromatized Al Kα radiation (1486.6 eV). The XPS peaks are then matched into sub-components using a Gaussian (80%)-Lorentzian (20%) curve-fitting program (XPSPEAK 4.1). Peaks at 398.8 ± 0.2, 399.8 ± 0.3, 400.4 ± 0.2, 401.4 ± 0.2 and 402–405 eV are used for the curve resolution [28]. Based on the previous studies [34,35], these peaks are assigned for pyridinic-N, amino-N/amide-N/amine-N, pyrrolic-N, quaternary-N and oxide-N, respectively. The content of each nitrogen-containing functionality in char ($Y_{N_{i,\ carbon}}$) is determined by the ratio of its corresponding peak area to the sum of peak areas (see Eq. (1)).

$$Y_{N_{i,carbon}} = \frac{A_{N_{i,carbon}}}{\sum A_{N_{i,carbon}}} \quad (1)$$

Where $A_{N_{i,\ carbon}}$ is peak area of each nitrogen functionality in XPS spectra.

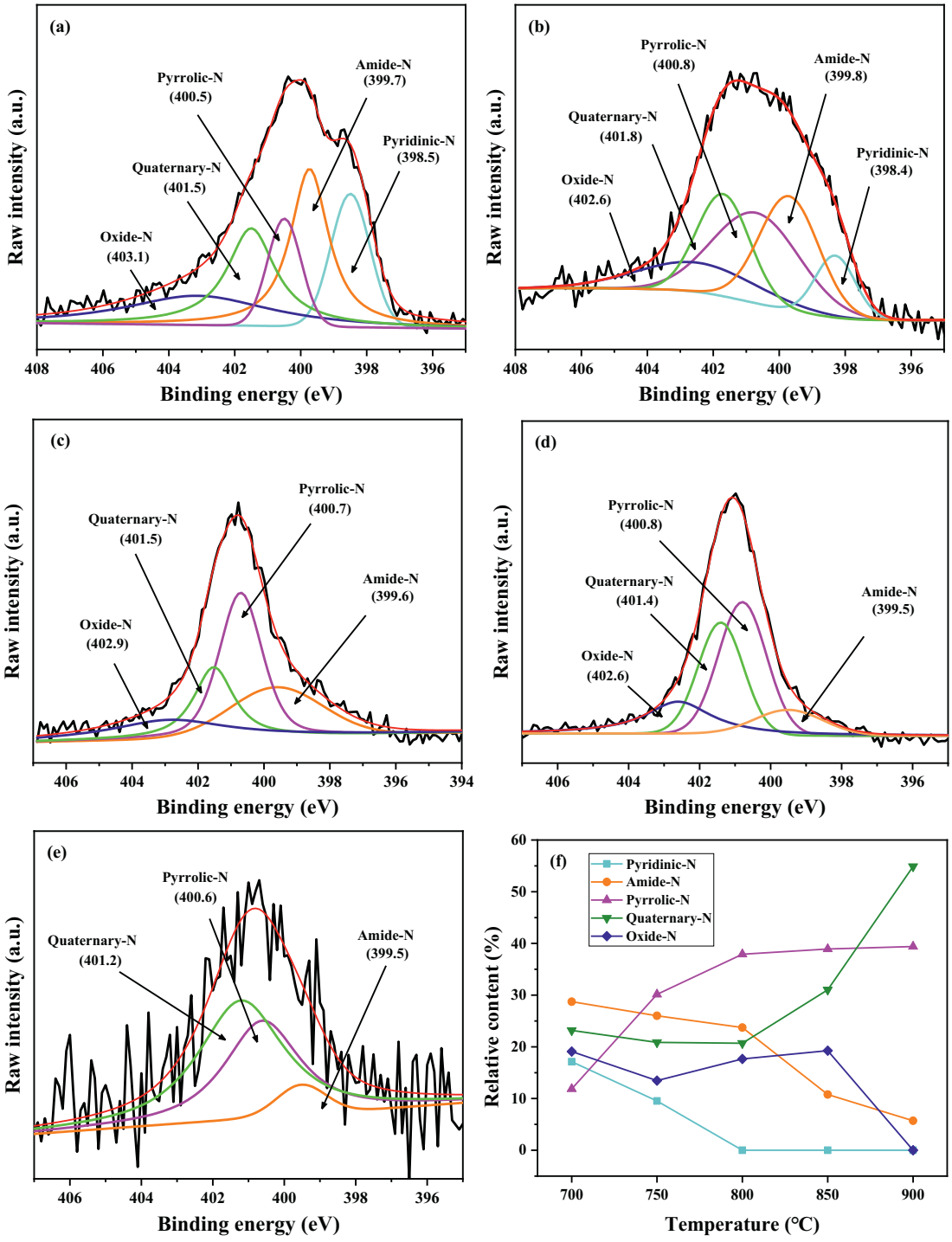

Fig. 4. High-resolution XPS N1s spectra of char: (a) B-700, (b) B-750, (c) B-800, (d) B-850, (e) B-900; And (f) relative content of XPS N 1 s peaks.

3. Results and discussion

3.1. Nitrogen distribution in raw algae

The XPS N 1 s spectra of raw algae is shown in Fig. S2. It is fitted into two peaks, protein-N/amine-N/amide-N (399.8 ± 0.3 eV) and inorganic-N (401.5 ± 0.3 eV, ammonia-N [NH_4^+] and nitrates-N/nitrites-N [NO_3^-/NO_2^-]). Protein-N is the major N-containing functional group with a relative content of about 97.8 wt.% in algae.

The detail composition of protein nitrogen is further analyzed by the L8800 automated amino acid analyzer, and a total of 17 amino acids are detected as shown in Table S1. The six major amino acids are glutamic acid (7.07 wt.%), aspartic acid (4.97 wt.%), leucine (4.67 wt.%), alanine (3.67 wt.%), proline (3.61 wt.%) and isoleucine (3.54 wt.%), accounting for over 50% in 17 amino acids. In addition, the total amino acids contents (53.06 wt.%) is slightly lower than proteins contents (59.35 wt. %, as reported in our previous study [35]), which is due to that some amino acids (e.g. tryptophan, methionine) could not be detected by the analyzer.

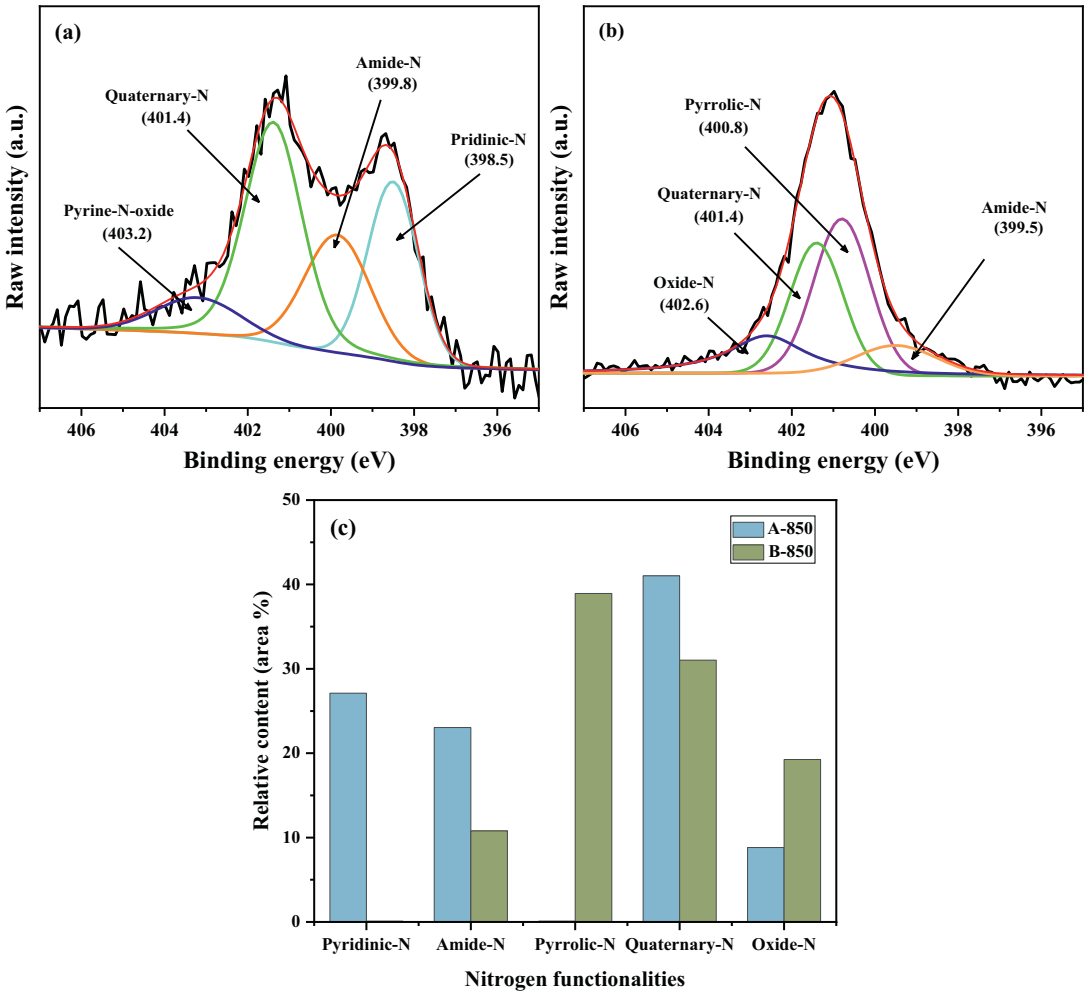

Fig. 5. High-resolution XPS N1s spectra of char: (a) A-850, (b) B-850; And (c) relative content of XPS N 1 s peaks.

3.2. Nitrogen distribution in pyrolysis products and molten salt

The overall mass balance of char, oil and gas from pyrolysis in molten salt is shown in Fig. S3. In order to ensure the accuracy of data, the experimental results for char, bio-oil and gas have been validated by reproducibility trials. With the increase of temperature, the solid yield gradually decreased, while the yield of bio-oil and gas increased. The amount of nitrogen in char, bio-oil and gas is shown in Table S2. The N yields of pyrolysis products and molten salt at different temperatures are calculated by the ratio of nitrogen amount in the products to that of raw algae, and the results is shown in Fig. 1.

In the temperature range of 700 to 900 °C, nitrogen is mostly concentrated in gas (ranges from 43.1 wt.% to 75.7 wt.%), and char-N and bio-oil-N is always low, with the total content not exceeding 40%. The gas-N rises sharply with the increase of temperature, reaching 75.7 wt.% at 900 °C, while the N yields of other products show the opposite trend. It can be attributed to that the secondary cracking of N-containing intermediates in char and bio-oil leads to the formation of non-condensable gases [35,36]. The N yield in molten salt decreases with increasing temperature, suggesting that molten salt participates in the reaction with nitrogen-containing substances and has a certain capacity to fix nitrogen. However, this capacity decreases at higher temperatures, mainly because high temperatures promote the equilibrium reaction of CN- hydrolysis (mentioned in section 3.3). In the following sections, the properties and transformation of these nitrogen-containing compounds under different pyrolysis temperatures will be further discussed.

3.3. Nitrogen distribution and transformation in gas

The release characteristics of N-containing gas during algae pyrolysis with a final temperature of 900 °C with and without molten salt are presented in the Fig. 2. As shown in Fig. 2(a), the N-containing gas during conventional pyrolysis are mainly NH_3 and HCN with a small amount of NO. NH_3 mainly produced from the pyrolysis of protein-N/amide-N [29], and its release peak appears at around 500 °C. The release curve of HCN presents two peaks, which corresponds to the decomposition of nitriles and the second cracking of pyridine-N in char, respectively [37]. In addition, a small amount of NO is generated under an inert environment, which is reported to be the decomposition of nitrate/nitrite and oxygenated organic matter [38]. In the presence of molten salt (show in Fig. 2(b)), the release peaks of NH_3 and NO are all advanced due to the catalytic performance of molten salt. The mass of N-containing gases during pyrolysis with and without molten salt is presented in Table S3. The amount of HCN decreased by 89.6% mainly due to the reaction with molten salt (see Reaction 2). In addition, the amount of NH_3 and NO is increased, mainly due to Na^+/K^+ in molten salt promoting the decomposition of amino acids to NH_3, while it enhances the reaction of nitrogen containing compounds and OH radicals to form NO [27,37].

$$K_2CO_{3(l)} + HCN_{(g)} \rightarrow 2KCN_{(l)} + H_2O_{(g)} + CO_{2(g)} \Delta G_{923K} = -1172.4kJ \quad (2)$$

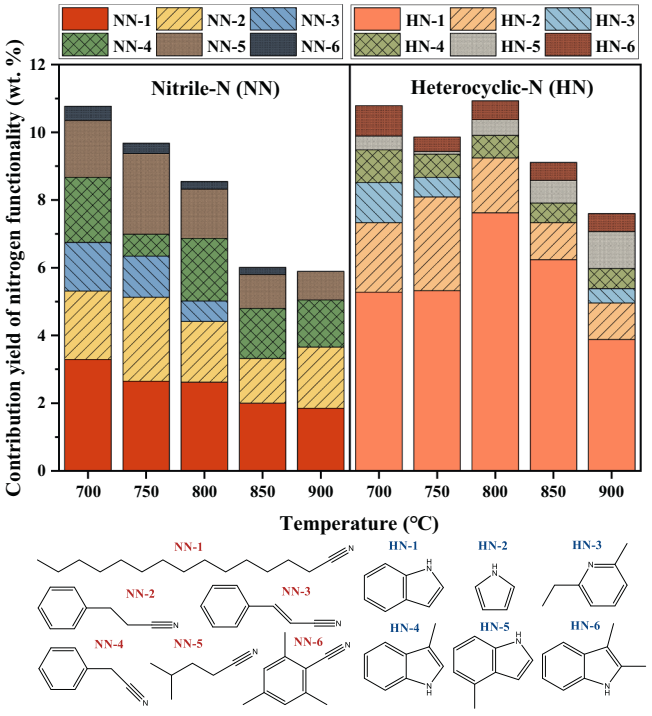

Fig. 6. Contribution of each nitrogen functionality in molten salt pyrolysis bio-oil vs. the temperature.

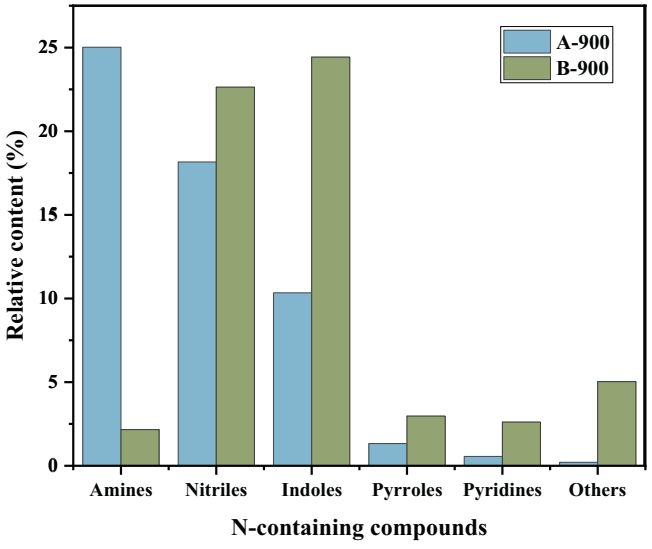

Fig. 7. N-containing compounds in bio-oil produced at different reaction medium.

3.4. Nitrogen distributions in molten salt

The composition of molten salt before and after reaction is detected to further examine the effect of molten Na_2CO_3-K_2CO_3 on the evolution of gas—N. The XPS N 1 s spectra is shown in Fig. 3. It can be seen that the molten salt after reaction contains a certain amount of CNO^- [39] and CN^- [40], which is not existed in the molten salt before reaction, suggesting that molten salt participates in the reaction with gas-N during algae pyrolysis. The main source of CN^- is the reaction between HCN and molten salt (see Reaction 2), and the CNO^- is most likely because the CN^- is oxidized during the XPS test (see Reaction 3).

$$2NaCN_{(s)} + O_{2(g)} \rightarrow 2NaCNO_{(s)} \Delta G_{303K} = -553.4kJ \quad (3)$$

3.5. Nitrogen distribution and transformation in char

The XPS N 1 s spectra and relative content of each nitrogen functionality are presented in Fig. 4. The inorganic-N (ammonia-N and nitrates-N/nitrites-N) in char disappeared compared with that of raw algae. It is because inorganic-N has poor thermal stability and decomposes at temperature around 300 °C, leading to the release of NH_3 and NO, as shown in Reaction 4–5 and Fig. 2(b) [29,38]. The protein-N in raw algae is largely converted to amide-N, pyridinic-N, pyrrolic-N, quaternary-N and oxide-N, which coexist as an interconnected structure in char as presented in Fig. S4.

$$NH_4^+ \rightarrow NH_3 + H^+ \quad (4)$$

$$NO_3^- / NO_2^- \rightarrow NO \quad (5)$$

Pyrrolic-N and pyridinic-N account for approximately 11.87% and 17.12% in char-N at 700 °C. As temperature rises from 700 °C to 800 °C, the pyrrolic-N increased sharply, while the pyridinic-N decreased rapidly until it disappeared. It is because higher temperatures enhance the interaction of amino acids (such as aspartic acid and glutamic acid) to form five-membered nitrogen rings by direct cyclization or dimerization, increasing the pyrrolic-N content [41]. Meanwhile, higher temperatures may also promote the conversion of pyridinic-N to pyrrolic-N [42]. The content of quaternary-N remains at about 23% at temperature of 700–800 °C, and increased sharply to 54.88% at 900 °C. Amide-*N* and pyrrolic-N are converted into quaternary-N, which has a more stable N-heterocyclic structure at higher temperatures [30]. In detail, amide-N continues to decompose into quaternary-N, and pyrrolic-N at char molecular boundary can be clogged into grapheme layers and converted to quaternary-N [29,43]. The content of oxide-N changes little (15–20%) over the temperature range of 700–850 °C, but decreases sharply to zero at 900 °C. Li et al. concluded that oxide-N is formed by pyridine-N bonded with oxygen-containing functional groups, while the N—O bond breaks at higher temperatures [30], which corresponds to the release of NO at higher temperatures shown in Fig. 2 (b).

Fig. 5 shows the high-resolution XPS N1s spectra of char prepared by pyrolysis and molten salt pyrolysis of algae at 850 °C. It can be found that A-850 contains pyridinic-N (around 28%) but no pyrrolic-N, and B-850 contains a large amount of pyrrolic-N but no pyridinic-N, while the content of other N-containing functional groups is not significantly different. It indicates that molten salt greatly promotes the formation of pyrrolic-N mainly from pyridinic-N. The content of amide-N in A-850 decreased by about half compared to that of B-850 mainly due to that the catalytic effect of molten salt intensifies the decomposition of it. In addition, the oxide-N content in B-850 is approximately double than that of A-850. Molten salt can provide free oxide ion (O^{2-}) through the Reaction 6, which favors the oxide-N formation [44].

$$CO_3^{2-} \rightarrow CO_2 + O^{2-} \quad (6)$$

3.6. Nitrogen distribution and transformation in bio-oil

The N-containing compounds detected by GC–MS are classified into amine-N, nitrile-N and heterocyclic-N (pyrrole/indole/pyridine compounds). The composition and relative content of these species is shown in Table S4. Nitriles and N-heterocyclic compounds are the main components, accounting for 35.70–57.51% and 39.53–50.53% of the N-containing species in bio-oil obtained, respectively.

As the temperature rises, the nitriles content decreases slightly by roughly 5% at 850 °C, mainly due to the decomposition of nitriles to form HCN. Kim [45] and Chen et al. [35] pointed that each nitrile-N species is largely produced from the evolution of amino acid or

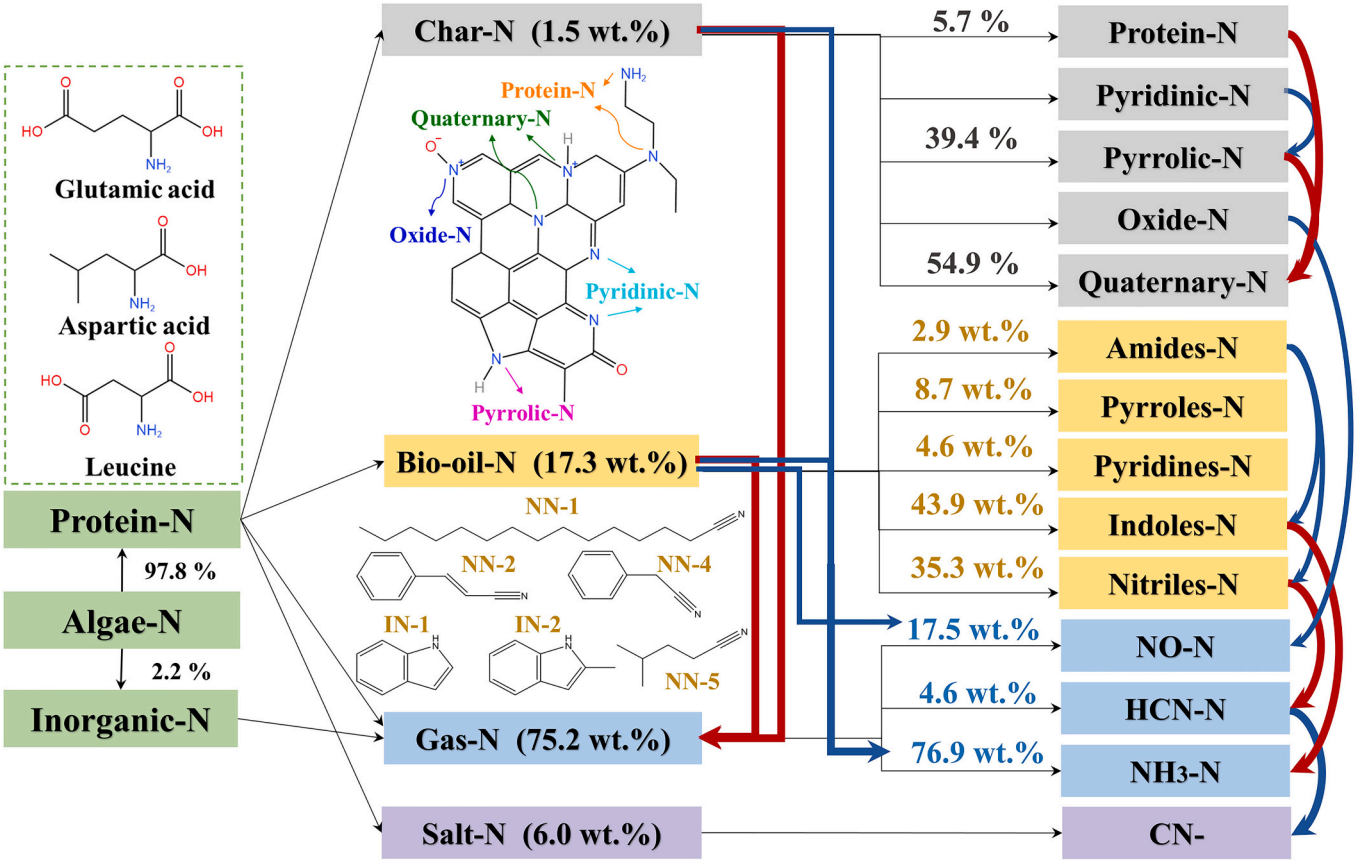

Fig. 8. Nitrogen transformation during algae pyrolysis in molten salt at 700–900 °C (black line: composition or reaction pathway, red line: promoted at high temperatures, blue line: promoted by molten salt, line width: conversion intensity). (For interpretation of the references to colour in this figure legend, the reader is referred to the web version of this article.)

amines containing corresponding branched chain. It is possible to speculate that short-chain nitriles (isoamyl cyanide) and nitriles with heterocyclic rings (benzenepropanenitrile) are mainly generated from leucine and aromatic amino acids like phenylalanine, respectively. Long-chain nitriles may come from the fatty acids generated from decomposition of triglycerides in algae, which firstly react with NH_3/NH_2^- to form long chain amides such as pentadecylamine and then dehydrate to form long chain nitriles (pentadecanenitrile) [45,46]. The content of N-heterocyclic compounds increases as the temperature increases from 700 °C to 800 °C, which is consistent with the existing studies [35]. However, as the temperature continues to rise, the N-heterocyclic decreases due to its decomposition to form NH_3. Indole compounds are the main components of N-heterocyclic compounds, and they can occupy more than 65% of N-heterocyclic compounds at 700–900 °C. The dehydrogenation, decarboxylation and dehydration of phenylalanine or tyrosine fragments may lead to the formation of indole compounds [46].

The contribution of each N-containing compound in the above two major species to bio-oil-N yield (Y_{N_i}) is calculated using Eq. (7) to clary the distribution of nitrogen in bio-oil [47], and the results is presented in Fig. 6.

$$Y_{N_i} = \frac{m_{bio-oil-N}}{m_{sample-N}} \left(\frac{A_i}{A_{all}} \cdot \frac{14.01 \cdot n_i}{M_i} \right) \Big/ \sum_i \left(\frac{A_i}{A_{all}} \cdot \frac{14.01 \cdot n_i}{M_i} \right) \tag{7}$$

Where $m_{bio-oil-N}$ and $m_{sample-N}$ are the nitrogen weight in bio-oil and raw algae, respectively; A_{all} and A_i are the area of the total chromatogram peaks and the target N-containing compound; n_i and M_i are the nitrogen atom number and the molecular weight of target N-containing compound.

It is revealed in Fig. 6 that for nitrile-N, although NN-1 makes up more than 10% of the compound in bio-oil, its contribution to the bio-oil-N yield is comparable to that of NN-2, NN-4 and NN-5. And for heterocyclic-N, HN-1 and HN-2 are the main contributing components to the bio-oil-N yield. It implies that studies of nitrogen conversion in bio-oil should not only focus on compounds with high content, but also include the contribution to bio-oil-N. The contribution of nitriles to bio-oil-N yield decreases due to their decomposition at higher temperatures. In contrast, the contribution of N-heterocyclic compounds to bio-oil-N yield only decreases slightly above 800 °C, suggesting that N-heterocyclic compounds are more stable at higher temperatures.

To further illustrate the role of molten salt in the regulation of nitrogen-containing compounds in bio-oil, the content of associated N-containing compounds obtained at different reaction medium at 900 °C is shown in Fig. 7. In the present of molten salt, only the amines content decreases, the rest of nitrogen-containing compounds increases to some extent, among which indoles increase by up to 15%. This may suggest that molten carbonates promote the dehydration or deamination of amides, while intensify the dehydrogenation, decarboxylation and dehydration of amino acids (phenylalanine and tyrosine) to form pyrroles.

3.7. Nitrogen transformation during the algae pyrolysis in molten carbonates

Based on the above discussions, the nitrogen transformation during algae pyrolysis in molten Na_2CO_3-K_2CO_3 is presented in Fig. 8. Algae-N, containing 97.8% protein-N and 2.2% inorganic-N, is mainly converted to gas-N (75.2 wt.%), followed by bio-oil-N (17.3 wt.%), salt-N (6.0 wt.%) and char-N (1.5 wt.%) at 900 °C. As the temperature rises, the bio-oil-

N and char-N are gradually converted into gas—N. The gas-N primally contains NH_3 (76.9 wt.%%), HCN (4.6 wt.%) and NO (17.5 wt.%). Molten salt reduces the HCN amount by 89.6%, trapping HCN as CN^- (salt-N), and increases the amount of NH_3 and NO mainly through the decomposition of bio-oil-N and char-N, as well as the reaction between N-containing species and OH radicals. The char-N is made up of amide-N (5.7%), pyridinic-N (0%), pyrrolic-N (39.4%), quaternary-N (54.9%) and oxide-N (0%). The higher temperature enhances the conversion of protein-N/amide-N and pyrrolic-N to quaternary-N, and the molten salt promotes the formation of pyridinic-N and NO from pyridinic-N and oxide-N, respectively. The bio-oil-N mainly consists of amine-N (2.9 wt.%), nitrile-N (35.3 wt.%) and heterocyclic-N (57.2 wt.%). The decomposition of nitriles-N and indoles-N is intensified at higher temperature to form HCN and NH_3, while the molten salt in turn promotes the formation of nitrile-N and indole-N from amide-N.

4. Conclusion

Algae-N is mainly converted to gas—N, followed by bio—N, salt-N and char-N. As the temperature rises, the gas-N yield increases (up to 75.7 wt.% at 900 °C), while the rest show a downward trend. For N-containing gas, the release temperature of all gas is reduced due to the catalytic effect of molten salt. HCN yield is inhibited by up to 89.6%, but the release of NH_3 and NO is promoted. For molten salt, nitrogen is mainly retained by its reaction with HCN to form CN^-. For N-containing char, protein-N decomposes mainly into amide-N, pyridine-N, pyrrole-N, quaternary-N and oxidized-N at lower temperatures (700–800 °C). At 800–900 °C, char-N is composed mainly of pyrrole-N and quaternary-N, mainly because molten salt promotes the formation of pyrrole-N, while quaternary-N is more stable at high temperatures. For N-containing bio-oil, nitriles and N-heterocyclic compounds are the primary components, accounting for 35.70–57.51% and 39.53–50.53%, respectively under different temperatures. Pentadecanenitrile, cinnamonitrile, benzyl nitrile and isoamyl cyanide in nitrile, as well as indole and pyrrole in N-heterocyclic, are the major contributing components to the bio-oil-N yield. Molten salt promotes the dehydration or deamination of amides and the formation of pyrroles. It is suggested to pay attention to the application of indole and nitrile as valuable products during the value-added carbon production, and to control the release of pollution gases such as NH_3 and NO.

CRediT authorship contribution statement

Jing Peng: Writing – original draft. **Jun Li:** Software, Visualization, Writing – review & editing. **Dian Zhong:** Investigation, Formal analysis. **Kuo Zeng:** Formal analysis, Conceptualization. **Kang Xu:** Software, Visualization. **Junjie Gao:** Software. **Ange Nzihou:** Methodology, Formal analysis. **Xiong Zhang:** Formal analysis, Validation. **Haiping Yang:** Resources, Validation. **Hanping Chen:** Validation.

Declaration of Competing Interest

The authors declare that they have no known competing financial interests or personal relationships that could have appeared to influence the work reported in this paper.

Data availability

The authors declare that the data supporting the findings of this study are available within the paper and its Supplementary information files. Extra data are available from the corresponding author upon request.

Acknowledgement

Authors acknowledge funding from the National Natural Science Foundation of China (52111530296, 52076098) and The Young Top-notch Talent Cultivation Program of Hubei Province. Authors would like to thank the Analytical and Testing Center in Huazhong University of Science & Technology (http://atc.hust.edu.cn) and the shiyanjia lab (https://www.shiyanjia.com) for the test. There are no conflicts to declare.

Appendix A. Supplementary data

Supplementary data to this article can be found online at https://doi.org/10.1016/j.fuproc.2023.107664.

References

[1] T.Y.A. Fahmy, Y. Fahmy, F. Mobarak, M. El-Sakhawy, R.E. Abou-Zeid, Biomass pyrolysis: past, present, and future, Environ. Dev. Sustain. 22 (2020) 17–32.
[2] S. Pourkarimi, A. Hallajisani, A. Alizadehdakhel, A. Nouralishahi, Biofuel production through micro- and macroalgae pyrolysis – a review of pyrolysis methods and process parameters, J. Anal. Appl. Pyrolysis 142 (2019), 104599.
[3] S.V. Vassilev, C.G. Vassileva, Composition, properties and challenges of algae biomass for biofuel application: an overview, Fuel 181 (2016) 1–33.
[4] W. Chen, B. Lin, M. Huang, J. Chang, Thermochemical conversion of microalgal biomass into biofuels: a review, Bioresour. Technol. 184 (2015) 314–327.
[5] D.V. Suriapparao, H.K. Tanneru, B.R. Reddy, A review on the role of susceptors in the recovery of valuable renewable carbon products from microwave-assisted pyrolysis of lignocellulosic and algal biomasses: prospects and challenges, Environ. Res. 215 (2022), 114378.
[6] Y. Qian, P. Liu, H. Zhuang, L. Chen, L. Jia, J. Yang, Y. Pan, Y. Chen, Study on the reaction mechanism of nitrogenous compounds in zeolite-catalyzed pyrolysis of blue-green algae, Fuel Process. Technol. 236 (2022), 107413.
[7] W. Chen, P. Kuo, A study on torrefaction of various biomass materials and its impact on lignocellulosic structure simulated by a thermogravimetry, Energy 35 (2010) 2580–2586.
[8] E. Suali, R. Sarbatly, Conversion of microalgae to biofuel, Renew. Sust. Energ. Rev. 16 (2012) 4316–4342.
[9] D. Xu, G. Lin, S. Guo, S. Wang, Y. Guo, Z. Jing, Catalytic hydrothermal liquefaction of algae and upgrading of biocrude: a critical review, Renew. Sust. Energ. Rev. 97 (2018) 103–118.
[10] S. Sobek, Q.K. Tran, R. Junga, S. Werle, Hydrothermal carbonization of the waste straw: a study of the biomass transient heating behavior and solid products combustion kinetics, Fuel 314 (2022), 122725.
[11] J.A.D. Juan Carlos Serrano-Ruiz, Catalytic routes for the conversion of biomass into liquid hydrocarbon transportation fuels, Energy Environ. Sci. (2011) 83–99.
[12] K. Xu, J. Li, K. Zeng, D. Zhong, J. Peng, Y. Qiu, G. Flamant, H. Yang, H. Chen, The characteristics and evolution of nitrogen in bio-oil from microalgae pyrolysis in molten salt, Fuel 331 (2023) 125903.
[13] H.Y. Zuo, K. Zeng, D. Zhong, J. Li, Y. Qiu, H.Q. Xu, G. Flamant, H.P. Yang, H. P. Chen, Multi-dimensional shrinkage models developed by phase field method for gasification of carbonaceous feedstock in packed-bed solar reactor, Fuel 331 (2023) 125749.
[14] J. Chen, J. Liang, Z.J.E. Xu, Assessment of supercritical water gasification process for combustible gas production from thermodynamic, environmental and techno-economic perspectives: a review, Energ. Convers. Manage. 226 (2020) 113497.
[15] Q. Guo, B. Yan, Y. Hu, Z. Cheng, R. Zhang, G. Chen, L. Hou, Biomass gasification ash reutilization: recirculation reusability and mechanism analysis, Waste Manag. 154 (2022) 64–73.
[16] D. Wu, J. Hu, C. Zhu, J. Zhang, H. Jing, C. Hao, Y. Shi, Salt melt synthesis of chlorella-derived nitrogen-doped porous carbon with atomically dispersed con4 sites for efficient oxygen reduction reaction, J. Colloid Interface Sci. 586 (2021) 498–504.
[17] H. Yin, B. Lu, Y. Xu, D. Tang, X. Mao, W. Xiao, D. Wang, A.N. Alshawabkeh, Harvesting capacitive carbon by carbonization of waste biomass in molten salts, Environ. Sci. Technol. 48 (2014) 8101–8108.
[18] S. Rawat, R.K. Mishra, T. Bhaskar, Biomass derived functional carbon materials for supercapacitor applications, Chemosphere 286 (2022), 131961.
[19] B. Li, J. Tang, X. Xie, J. Wei, D. Xu, L. Shi, K. Ding, S. Zhang, X. Hu, S. Zhang, D. Liu, Char structure evolution during molten salt pyrolysis of biomass: effect of temperature, Fuel 331 (2023), 125747.
[20] Y. Gao, R. Sun, A. Li, G. Ji, In-situ self-activation strategy toward highly porous biochar for supercapacitors: direct carbonization of marine algae, J. Electroanal. Chem. 882 (2021), 114986.
[21] B. Lu, L. Hu, H. Yin, X. Mao, W. Xiao, D. Wang, Preparation and application of capacitive carbon from bamboo shells by one step molten carbonates carbonization, Int. J. Hydrogen Energ. 41 (2016) 18713–18720.
[22] B. Lu, L. Hu, H. Yin, W. Xiao, D. Wang, One-step molten salt carbonization (msc) of firwood biomass for capacitive carbon, RSC Adv. 6 (2016) 106485–106490.
[23] Y. Liu, X. Cheng, S. Zhang, One-step molten salt carbonization of tobacco stem for capacitive carbon, J. Porous. Mater. 28 (2021) 1629–1642.
[24] X. He, K. Zeng, Y. Xie, G. Flamant, H. Yang, X. Yang, A. Nzihou, A. Zheng, Z. Ding, H. Chen, The effects of temperature and molten salt on solar pyrolysis of lignite, Energy 181 (2019) 407–416.

[25] J. Li, Z. Xiong, K. Zeng, D. Zhong, X. Zhang, W. Chen, A. Nzihou, G. Flamant, H. Yang, H. Chen, Characteristics and evolution of nitrogen in the heavy components of algae pyrolysis bio-oil, Environ. Sci. Technol. 55 (2021) 6373–6385.
[26] L. Xu, Q. Yao, J. Deng, Z. Han, Y. Zhang, Y. Fu, G.W. Huber, Q. Guo, Renewable n-heterocycles production by thermocatalytic conversion and ammonization of biomass over zsm-5, ACS Sustain. Chem. Eng. 3 (2015) 2890–2899.
[27] H. Chen, R. Shan, F. Zhao, J. Gu, Y. Zhang, H. Yuan, Y. Chen, A review on the nox precursors release during biomass pyrolysis, Chem. Eng. J. 451 (2023), 138979.
[28] H. Zhan, X. Zhuang, Y. Song, X. Yin, C. Wu, Insights into the evolution of fuel-n to nox precursors during pyrolysis of n-rich nonlignocellulosic biomass, Appl. Energy 219 (2018) 20–33.
[29] Y. Tian, J. Zhang, W. Zuo, L. Chen, Y. Cui, T. Tan, Nitrogen conversion in relation to nh3 and hcn during microwave pyrolysis of sewage sludge, Environ. Sci. Technol. 47 (2013) 3498–3505.
[30] L.L.T. Chun-Zhu Li, Formation of nox and sox precursors during the pyrolysis of coal and biomass. Part iii. Further discussion on the formation of hcn and nh3 during pyrolysis, Fuel 15 (2000) 1899–1906.
[31] Y. Wei, J. Tang, J. Ji, The characteristics of products from pyrolysis of seaweed in molten carbonates, T. Asabe 62 (2019) 787–794.
[32] K. Xu, J. Li, K. Zeng, D. Zhong, J. Peng, Y. Qiu, G. Flamant, H. Yang, H. Chen, The characteristics and evolution of nitrogen in bio-oil from microalgae pyrolysis in molten salt, Fuel 331 (2023), 125903.
[33] K. Zeng, J. Li, Y. Xie, H. Yang, X. Yang, D. Zhong, W. Zhen, G. Flamant, H. Chen, Molten salt pyrolysis of biomass: the mechanism of volatile reforming and pyrolysis, Energy 213 (2020), 118801.
[34] H. Liu, G. Luo, H. Hu, Q. Zhang, J. Yang, H. Yao, Emission characteristics of nitrogen- and sulfur-containing odorous compounds during different sewage sludge chemical conditioning processes, J. Hazard. Mater. 235-236 (2012) 298–306.
[35] W. Chen, H. Yang, Y. Chen, M. Xia, X. Chen, H. Chen, Transformation of nitrogen and evolution of n-containing species during algae pyrolysis, Environ. Sci. Technol. 51 (2017) 6570–6579.
[36] L. Wei, L. Wen, T. Yang, N. Zhang, Nitrogen transformation during sewage sludge pyrolysis, Energy Fuel 29 (2015) 5088–5094.
[37] K. Tian, W. Liu, T. Qian, H. Jiang, H. Yu, Investigation on the evolution of n-containing organic compounds during pyrolysis of sewage sludge, Environ. Sci. Technol. 48 (2014) 10888–10896.
[38] H. Liu, Q. Zhang, H. Hu, P. Liu, X. Hu, A. Li, H. Yao, Catalytic role of conditioner cao in nitrogen transformation during sewage sludge pyrolysis, P. Combust. Inst. 35 (2015) 2759–2766.
[39] B. Mavis, M. Akinc, Cyanate intercalation in nickel hydroxide, Chem. Mater. 18 (2006) 5317–5325.
[40] Q. Zhao, H. Yang, L. Tong, Adsorption characteristics of cn− species on the chalcopyrite surface and its response to flotation, Sep. Purif. Technol. 276 (2021), 119322.
[41] J.R. Pels, F. Kapteijn, J.A. Moulijn, Q. Zhu, K.M. Thomas, Evolution of nitrogen functionalities in carbonaceous materials during pyrolysis, Carbon 33 (1995) 1641–1653.
[42] C. Guo, C. Chen, Z. Luo, A novel nitrogen-containing electrocatalyst for oxygen reduction reaction from blood protein pyrolysis, J. Power Sources 245 (2014) 841–845.
[43] M. Xu, S. Li, Y. Wu, L. Jia, Q. Lu, Effects of co2 on the fuel nitrogen conversion during coal rapid pyrolysis, Fuel 184 (2016) 430–439.
[44] S. Frangini, A. Masi, Molten carbonates for advanced and sustainable energy applications: part i. Revisiting molten carbonate properties from a sustainable viewpoint, Int. J. Hydrogen Energ. 41 (2016) 18739–18746.
[45] S.W. Kim, B.S. Koo, D.H. Lee, A comparative study of bio-oils from pyrolysis of microalgae and oil seed waste in a fluidized bed, Bioresour. Technol. 162 (2014) 96–102.
[46] O. Debono, A. Villot, Nitrogen products and reaction pathway of nitrogen compounds during the pyrolysis of various organic wastes, J. Anal. Appl. Pyrolysis 114 (2015) 222–234.
[47] H. Zhan, X. Yin, Y. Huang, H. Yuan, C. Wu, Nox precursors evolving during rapid pyrolysis of lignocellulosic industrial biomass wastes, Fuel 207 (2017) 438–448.